

Optical design of inhomogeneous media to perfectly focus scalar wave fields

Pablo Benítez^{*}, Juan C. Miñano, Juan C. González

Universidad Politécnica de Madrid, Cedint, Campus de Montegancedo 28223, Madrid, Spain

ABSTRACT

A method to design isotropic inhomogeneous refractive index distribution is presented, in which the scalar wave field solutions propagate exactly on an eikonal function (*i.e.*, remaining constant on the Geometrical Optics wavefronts). This method is applied to the design of “dipole lenses”, which perfectly focus a scalar wave field emitted from a point source onto a point absorber, in both two and three dimensions. Also, the Maxwell fish-eye lens in two and three dimensions is analyzed.

Keywords: Inhomogeneous optical media, Gradient-index lenses, Helmholtz equation

1. INTRODUCTION

It is common to deduce Geometrical Optics as a limit case of Scalar Wave Optics, for instance, when the wavenumber $k=\omega/c$ is very large. In that limit, the propagation of the scalar field can be calculated with good approximation using rays. There are, however, some trivial cases in which the ray trajectories guide the scalar field in an exact manner (*i.e.* with no restriction to large k) so that the field is constant on the Geometrical Optics wavefronts. For instance, a (monopole) point source emitting from the center of a spherical symmetric refractive index distribution $n(\mathbf{r})$ will generate a field which will depend on the radial coordinate only. In this paper we are going to discuss about isotropic inhomogeneous refractive index distributions that propagate nontrivial scalar fields exactly on eikonals (*i.e.*, remaining constant on the Geometrical Optics wavefronts), and we will find media that produce perfect focusing of rays and waves, perfect in the sense explained next.

In Geometrical Optics, an optical system is said to produce a perfect focus (or sharp image) of an object point \mathbf{P} onto an image point \mathbf{Q} when any ray trajectory emitted from \mathbf{P} through the optical system will pass through \mathbf{Q} in an exact way. Such points \mathbf{P} and \mathbf{Q} are said to be perfect conjugates [1]. A device is called an Absolute Instrument in Geometrical Optics if it produces perfect focusing of rays not just from a single object point, but of all points in a three-dimensional domain (*i.e.*, one with non-null volume) [1].

The ellipsoidal mirror is a well known example of perfect focusing of rays, but only for points \mathbf{P} and \mathbf{Q} coincident with the foci of the ellipsoid (*i.e.*, it is not an Absolute Instrument). Non-trivial examples of Absolute Instruments are based on non-homogeneous media [2], the most famous being the Maxwell fish-eye lens [1]. Unlike conventional imaging optics systems, in the Maxwell fish-eye lens the refractive index in the volume containing the object and image points is inhomogeneous, (*i.e.*, spatially varying). There are, however, examples of Absolute Instruments in which the refractive index distribution in that volume is homogeneous [3].

An analogous concept to the performance of an Absolute Instrument in Scalar Wave and Electromagnetic Optics has been introduced by Pendry [4] in the field of metamaterials, under the rubric of Perfect Imaging, meaning image formation with unlimited resolution. It disclosed a specific device made of a negative refractive index slab with $n = \varepsilon = \mu = -1$, the capacity of which for perfect imaging has been explained by the amplification of evanescent waves in the negative index material.

Recently, Leonhardt [5] has proven that Perfect Imaging for 2D Helmholtz scalar fields is also achieved by the cylindrical Maxwell fish-eye lens, and the mirrored version referred to as the Maxwell fish-eye mirror. In three dimensions, Leonhardt and Philbin have proven very recently [6] that the spherical Maxwell fish eye lens is perfect for

* pablo.benitez@upm.es; phone +34 915441060; fax +34 915446341

focusing electromagnetic waves (not Helmholtz scalar wave fields) if the medium is impedance-matched ($n=\varepsilon=\mu$). These results are especially relevant because it uses isotropic positive refractive index.

The fact that the cylindrical Maxwell fish-eye lens is perfect for focusing both rays and scalar field waves in two dimensions is not a general result. For instance, even though the elliptic mirror is ideal for rays when \mathbf{P} and \mathbf{Q} coincide with the foci, it is well known that it does not focus waves perfectly (neither in two nor in three dimensions) due to the coma of the mirror.

In this paper we are going to discuss about the design of a class of isotropic inhomogeneous media that perfectly focus Helmholtz scalar field waves emitted from a point source at \mathbf{P} onto a point drain at \mathbf{Q} , problem that we introduced in [7]. This means that the local behavior of the field around \mathbf{Q} will coincide asymptotically with a spherical converging wave in three dimensions. In general, such a media will have no particular symmetry (nor spherical neither rotational). The two-dimensional case for cylindrical waves will be also considered.

Section 2 deals with the conditions that must be fulfilled for the Helmholtz scalar wave field to propagate exactly on an eikonal function, leading to a novel constructive design method. In section 3, this method is applied to cylindrical lenses, in particular to reproduce with a different approach the performance of the cylindrical Maxwell fish-eye in reference [5]. Section 4 will consider the three dimensional case, concluding with the design of a “3D dipole lens”, which perfectly focuses a point source \mathbf{P} upon a point drain \mathbf{Q} in three dimensions. Finally, Section 5 shows other examples with multiple sources or drains.

As a clarification, throughout this paper the term ‘Maxwell fish-eye’ will refer to the spatially unbounded refractive index distribution in the cylindrical and spherical symmetric cases, respectively, and not to the mirror bounded version discussed in references [3] and [5].

2. HELMHOLTZ FIELDS THAT PROPAGATE EXACTLY ON EIKONALS

2.1 Statement of the problem

Consider a scalar field $U(\mathbf{r}) \in X$, $\mathbf{r} \in \mathcal{D} \subset \mathbb{R}^3$ in a medium with refractive index distribution $n(\mathbf{r})$:

$$\Delta U(\mathbf{r}) + k^2 n^2(\mathbf{r})U(\mathbf{r}) = 0 \quad (1)$$

where $k=\omega/c$. As with [5] and [8], Eq.(1) is herein referred to as Helmholtz equation for inhomogeneous media (or just the Helmholtz equation for short) and its solution $U(\mathbf{r})$ is referred to a Helmholtz scalar wave field. Note that the name Helmholtz equation is sometimes reserved to the case $n=\text{constant}$ (i.e., the case of homogeneous media), while Eq.(1) is formally equivalent to the time-independent Schrödinger equation. This equation is relevant in other areas of physics, such as acoustics or optics. In optics, this equation in 2D is exact for describing TE polarized light in cylindrical media (in which electric field vector \mathbf{E} points orthogonal to the cross section of the cylinder). It is not exact but approximate, however, for describing electromagnetic fields in 3D.

Consider a function $S(\mathbf{r}) \in \mathcal{P}$ that is a particular solution of the eikonal equation in the domain \mathcal{D} .

$$(\nabla S)^2 = n^2(\mathbf{r}) \quad (2)$$

The integral curves of the vector field $\nabla S(\mathbf{r})$ are the geometrical optics rays associated with the eikonal function $S(\mathbf{r})$, which measures the advance of the optical path length along the rays. We can create the tri-orthogonal curvilinear coordinates (S,u,v) where u and v are the coordinates defined on the surfaces $S(\mathbf{r})=\text{constant}$. This coordinate system is used to express the transport equations in the Geometrical Optics approximation, and has been specifically used in Electromagnetic Optics by Stavroudis [9]. Additionally, it is also commonly applied in the method of characteristics for solving the time-dependent wave equation. In these new coordinates $S=S(\mathbf{r})$, $u=u(\mathbf{r})$, $v=v(\mathbf{r})$, Eq. (1) becomes:

$$(\nabla S)^2 \frac{\partial^2 U}{\partial S^2} + (\nabla u)^2 \frac{\partial^2 U}{\partial u^2} + (\nabla v)^2 \frac{\partial^2 U}{\partial v^2} + \Delta S \frac{\partial U}{\partial S} + \Delta u \frac{\partial U}{\partial u} + \Delta v \frac{\partial U}{\partial v} + k^2 n^2 U = 0 \quad (3)$$

Here $U=U(S,u,v)$ and $n=n(S,u,v)$. If there were solutions of U depending on S only, then (3) reduces to:

$$n^2 \frac{d^2U}{dS^2} + \Delta S \frac{dU}{dS} + k^2 n^2 U = 0 \quad (4)$$

For this to be possible, it must be that $\frac{\Delta S}{n^2} = F(S)$ (independent of u and v).

Given this, the field $U(S)$ will be a solution of the following ordinary differential equation:

$$\frac{d^2U}{dS^2} + F(S) \frac{dU}{dS} + k^2 U = 0 \quad (5)$$

Note that since $(\nabla S)^2 = n^2(\mathbf{r})$ we can state that there are solutions of U depending solely on S if (and only if) S fulfills:

$$\frac{\Delta S}{(\nabla S)^2} = F(S) \quad (\text{independent of } u \text{ and } v) \quad (6)$$

Note that any solution of Eq. (6) provides wavefronts for which $U=U(S)$ exists and the refractive index is calculated as $n(\mathbf{r}) = |\nabla S|$. As can be easily checked, Eq. (6) is also valid for two dimensions, *i.e.*, when the previous reasoning is followed with the Helmholtz equation (1) in two dimensions.

2.2 Solutions of Eq. (6)

We will prove next that a function S is a solution of functional equation (6) in the domain \mathcal{D} if and only if there is a real increasing function $V(S)$ which is harmonic in \mathcal{D} , *i.e.*, whose Laplacian is zero ($\Delta V=0$):

$$\Delta V = V_{SS} (\nabla S)^2 + V_S \Delta S = 0 \quad \Leftrightarrow \quad \frac{\Delta S}{(\nabla S)^2} = -(\ln V_S)_S \quad (7)$$

The function $F(S)$ of Eq (6) is thus

$$F(S) = -(\ln V_S)_S \quad (8)$$

Since V_S is the argument of a logarithm, it must be positive, which implies that $V(S)$ is monotonically increasing (and therefore invertible).

This solution gives a constructive method to calculate the refractive index distributions that propagate fields U exactly on eikonals. The design method comprises the following steps:

- Select a harmonic function $V(\mathbf{r})$ on \mathcal{D}
- Choose an increasing function $S(V)$
- Compute $F(S)$ via Eq. (8)
- Compute $n(\mathbf{r}) = |\nabla S|$

Field $U(\mathbf{r})$ can finally be obtained by solving Eq. (5) for $U(S)$, and then calculating $U(S(V(\mathbf{r})))$.

3. PERFECT FOCUSING IN TWO DIMENSIONS

3.1 The cylindrical Maxwell fish-eye lens

Consider first the cylindrical Maxwell fish-eye lens case with refractive index distribution:

$$n(\rho, z) = \frac{2aL}{a^2 + \rho^2} \quad (9)$$

Here L and a are positive real constants and ρ, z are cylindrical coordinates ($\rho^2=x^2+y^2$). As mentioned in the introduction, the Maxwell fish-eye lens is an Absolute Instrument in geometrical optics, and thus the rays contained in planes $z=z_0$ passing through any point \mathbf{P} will focus again at its conjugate point \mathbf{Q} . The position of \mathbf{Q} in the x - y plane can be obtained as the transformation from \mathbf{P} by an inversion with respect to the circle of radius a centered at \mathbf{O} , followed by central symmetry with respect to \mathbf{O} . Therefore, $\mathbf{P}\cdot\mathbf{Q} = -a^2$.

Leonhardt has recently proven in [5] that such ideality for focusing rays of the cylindrical Maxwell fish-eye lens also occurs for 2D Helmholtz fields. Leonhardt solved it by using the classical stereographic projection between the sphere and the plane, which Luneburg used as well to explain the ideality of the Maxwell fish-eye lens in ray optics [10]. We will confirm Leonhardt's result here by using the approach of the previous section: showing that the function S of the rays emitted from \mathbf{P} in the cylindrical Maxwell fish-eye lens fulfills Eq.(6).

Without loss of generality (due to the cylindrical symmetry), let us consider $\mathbf{P}=a(-\cosh \alpha - \sinh \alpha, 0, 0)$ and $\mathbf{Q}=a(\cosh \alpha - \sinh \alpha, 0, 0)$ for a given real constant α . Note that $\mathbf{P}\cdot\mathbf{Q} = -a^2\cosh^2\alpha + a^2\sinh^2\alpha = -a^2$. In the case $\alpha = 0$, $\mathbf{P}=(-a, 0, 0)$ and $\mathbf{Q}=(a, 0, 0)$.

Apply the following change of variables to the following decentered cylindrical bipolar coordinates (σ, τ, z) [11]:

$$\begin{aligned} x &= a \left(\cosh \alpha \frac{\sinh \tau}{\cosh \tau - \cos \sigma} - \sinh \alpha \right) \\ y &= a \cosh \alpha \frac{\sin \sigma}{\cosh \tau - \cos \sigma} \\ z &= z \end{aligned} \tag{10}$$

where $\sigma \in \left\{ -\frac{\pi}{2}, \frac{\pi}{2} \right\}$, $\tau, z \in \mathbb{R}$.

The cross section of surfaces of constant σ and constant τ are circles that intersect at right angles. As shown in Figure 1, curves of constant σ (in blue) correspond to circles that intersect at the two points \mathbf{P} and \mathbf{Q} , while the curves of constant τ (in red) are non-intersecting circles of different radii that surround the points \mathbf{P} and \mathbf{Q} . In this coordinate system, the gradient and Laplacian operators take the forms [11]:

$$\nabla = \left(\frac{\cosh \tau - \cos \sigma}{a \cosh \alpha} \frac{\partial}{\partial \sigma}, \frac{\cosh \tau - \cos \sigma}{a \cosh \alpha} \frac{\partial}{\partial \tau}, \frac{\partial}{\partial z} \right) \tag{11}$$

$$\Delta = \frac{(\cosh \tau - \cos \sigma)^2}{a^2 \cosh^2 \alpha} \left[\frac{\partial^2}{\partial \sigma^2} + \frac{\partial^2}{\partial \tau^2} \right] + \frac{\partial^2}{\partial z^2} \tag{12}$$

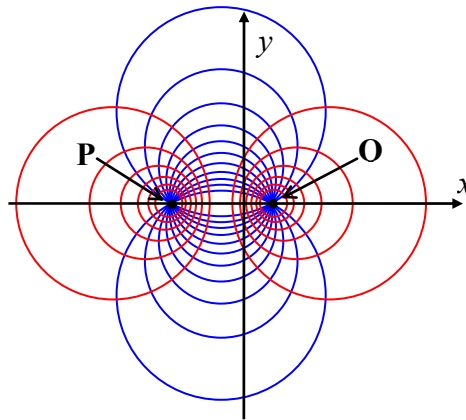


Figure 1. Cross section at $z=\text{constant}$ of the σ (in blue) and τ (in red) isosurfaces of the decentered cylindrical bipolar coordinate system.

The refractive index distribution of the Maxwell Fish Eye (Eq. (9)) is written in these coordinates (σ, τ, z) as:

$$n(\sigma, \tau, z) = \frac{L(\cosh \tau - \cos \sigma)}{a \cosh \alpha \cosh(\tau - \alpha)} \quad (13)$$

We can confirm that the τ isosurfaces coincide with Geometrical wavefronts by the fact that the eikonal equation $(\nabla S)^2 = n^2$ has particular solutions depending only on τ , *i.e.*, $S=S(\tau)$, which are calculated with Eq. (11) and Eq. (13):

$$\frac{dS}{d\tau} = \pm \frac{L}{\cosh(\tau - \alpha)} \Rightarrow S(\tau) = \pm 2L \arctan(\exp(\tau - \alpha)) + C \quad (14)$$

This utilizes the principal value of the arctangent function. Choose the solution with positive sign (so the optical path length S increases with τ) and $C=0$. The minimum value of $S(\tau)$ is reached at the **P** where $\tau \rightarrow -\infty$ and $S(-\infty)=0$, while the maximum value is achieved at the **Q** where $\tau \rightarrow \infty$ and $S(\infty)=\pi L$. Therefore $0 \leq S \leq \pi L$.

We can invert $S(\tau)$ to obtain:

$$\tau(S) = \alpha + \ln \left(\tan \left(\frac{S}{2L} \right) \right) \quad (15)$$

By (12):

$$\Delta S = \frac{(\cosh \tau - \cos \sigma)^2}{a^2 \cosh^2 \alpha} \frac{d^2 S}{d\tau^2} = -\frac{L}{a^2} \frac{(\cosh \tau - \cos \sigma)^2}{\cosh^2 \alpha} \frac{\sinh(\tau - \alpha)}{\cosh^2(\tau - \alpha)} \quad (16)$$

Then we can easily check that equation (6) is fulfilled, since:

$$\frac{\Delta S}{(\nabla S)^2} = -\frac{1}{L} \sinh(\tau - \alpha) = -\frac{1}{L} \sinh \left(\ln \left(\tan \left(\frac{S}{2L} \right) \right) \right) = \frac{1}{L \tan \left(\frac{S}{L} \right)} = F(S) \quad (17)$$

This uses Eq.(15). Therefore, there is a solution of the field U which is function of S only, and it fulfils the ordinary differential Eq. (5):

$$\frac{d^2 U}{dS^2} + \frac{1}{L \tan \left(\frac{S}{L} \right)} \frac{dU}{dS} + k^2 U = 0 \quad (18)$$

Using the change of variables $p = \tan \left(\frac{S}{2L} \right)$ (*i.e.*, $p = \exp(\tau - \alpha)$), we obtain:

$$\frac{d^2 U}{dp^2} + \frac{1}{p} \frac{dU}{dp} + (kL)^2 \left(\frac{2}{1+p^2} \right)^2 U = 0 \quad (19)$$

This is Equation (9) of reference [5], with the wavenumber scaled by the factor L (which was normalized to 1 in that reference). The resolution was described in detail there but is not pertinent and so will not be continued here.

$V(S)$ is obtained by integrating Eq. (8) with $F(S)$, given by Eq. (17) as:

$$V(S) = A \int \frac{dS}{\sin\left(\frac{S}{L}\right)} = AL \left(\ln \left(\tan \left(\frac{S}{2L} \right) \right) + B \right) = \tau(S) \quad (20)$$

Here the last equality is valid for $A=1/L$ and $B=\alpha$ (see Eq. (15)). This indicates that the function $\tau(x,y)$ is harmonic, which is in fact well known, since the mapping of the planes x - y to τ - σ produced by the bipolar coordinate transformation (10) is conformal [11], and therefore both $\tau(x,y)$ and $\sigma(x,y)$ are harmonic functions.

3.2 The general cylindrical case: The “2D dipole lens”

The method of section 2.2 can find a more general solution of a device that focuses perfectly the scalar waves emitted by a point source a \mathbf{P} at a point drain at \mathbf{Q} . For that task, consider again the following harmonic function in P^3 , valid except at the lines $x=-a; y=0$ and $x=a; y=0$

$$V(x, y, z) = \frac{1}{2} \ln \left(\frac{(x+a)^2 + y^2}{(x-a)^2 + y^2} \right) \quad (21)$$

This harmonic function is (up to a multiplicative constant) equal to the electrostatic potential created by an electric dipole with cylindrical symmetry along the z axis, *i.e.*, two line charges of equal magnitude but opposite sign crossing the $z=0$ plane on the points $\mathbf{P}=(-a,0,0)$ and $\mathbf{Q}=(a,0,0)$. The function (21) coincides with function $\tau(x,y)$ of the previous section for the case $\alpha=0$ (as can be checked by inverting the mapping (10)), which is well known in electrostatic theory [11].

According to the method described in section 2.2, we can select an arbitrary monotonic function $S(V)$. We will call this family of solutions the “2D dipole lens”. Different functions $S(V)$ lead to different refractive index distributions, but all of them have the same wavefronts and rays defined by the coordinate lines of the bipolar reference system (10). One distinguished solution of this family is the cylindrical Maxwell fish-eye lens discussed in the previous section. In general, the refractive index distribution will not be a function of ρ only, as was the case for the cylindrical Maxwell fish-eye lens. Also unlike the Maxwell fish-eye lens, a general 2D dipole lens will not produce perfect focusing of the cylindrical scalar waves emitted by a point source different than \mathbf{P} or \mathbf{Q} (which are focused one into the other). Therefore, no perfect imaging for a volumetric region is expected in the general case.

In the selection of $S(V)$ care must be taken with its asymptotic values when $|V| \rightarrow \infty$. This care is needed for the resulting refractive index (given by $|\nabla S|$) to be bounded, considering that V is unbounded around \mathbf{P} and \mathbf{Q} . In that case we must choose that when $|V| \rightarrow \infty$, *i.e.* for \mathbf{r} close to \mathbf{P} (or \mathbf{Q}):

$$n = |\nabla S| = S_V |\nabla V| \sim 1 \quad \Rightarrow \quad S_V \sim \frac{1}{|\nabla V|} \sim r \sim \exp(-|V|) \quad (22)$$

Here r denotes the distance from \mathbf{r} to \mathbf{P} (or \mathbf{Q}).

4. PERFECT FOCUSING IN THREE DIMENSIONS

Note that, in order to simplify the nomenclature, in this section the points \mathbf{P} and \mathbf{Q} are placed on the z axis, whereas in the previous section they were on the x axis.

We will see next that the “dipole lens” concept introduced in section 3.1 can be analogously defined in 3D, and it will lead to refractive index distributions which are not spherical symmetric but that produce the perfect focusing of the Helmholtz scalar wave field from \mathbf{P} to \mathbf{Q} in three dimensions. It must be noticed the spherical Maxwell fish eye lens, besides its ideal properties in Geometrical Optics, does not belong to the class of media discussed here in three dimensions, as proven in [7]. This means that there is not field that propagates on eikonals. Leonhardt and Philbin, however, have proven recently [6] that the spherical Maxwell fish eye lens can perfectly focus electromagnetic waves (not Helmholtz scalar wave fields) in three dimensions if the medium is impedance-matched ($n=\varepsilon=\mu$).

4.1 The general rotational case: The “3D dipole lens”

Consider the following harmonic function in \mathbb{P}^3 except at the points (x,y,z) given by $\mathbf{P}=(0,0,-a)$ and $\mathbf{Q}=(0,0,a)$ (so that $\mathcal{D} = \mathbb{R}^3 \setminus \{\mathbf{P}, \mathbf{Q}\}$)

$$V(\rho, z) = \frac{a}{\sqrt{\rho^2 + (z-a)^2}} - \frac{a}{\sqrt{\rho^2 + (z+a)^2}} \quad (23)$$

Here ρ, z are again cylindrical coordinates ($\rho^2=x^2+y^2$). This harmonic function is (up to a multiplicative constant) equal to the electrostatic potential created by an electric dipole (two point charges of equal magnitude but opposite sign) located on the points \mathbf{P} and \mathbf{Q} . That potential distribution has rotational symmetry with respect to the z axis, and the cross sections of the $V=\text{constant}$ surfaces and electrostatic field lines are shown in Figure 2 (see also an animation in [13]). In our case, the $V=\text{constant}$ surfaces are the wavefronts and the electrostatic field lines correspond to the ray trajectories and energy flux lines. Note that both families of curves are not circumferences, as occurred in the 2D case. Particularly, the $V=\text{constant}$ surfaces are ovals (8-degree algebraic curves) that belong to the family of Generalised Cayley’s ovals [14].

As in the 2D case, for the refractive index $n=|\nabla S|$ to be bounded, we must select $S(V)$ with the appropriate asymptotic behavior when $|V| \rightarrow \infty$, which in this 3D case is:

$$S_V \sim \frac{1}{|\nabla V|} \sim r^2 \sim |V|^{-2} \quad (24)$$

This is achieved for instance by the function:

$$S(V) = L \left(\frac{\pi}{2} + \arctan(V) \right) \quad (25)$$

Here again the principal value of the function \arctan is used. The minimum value of $S(\rho, z)$ is only reached at \mathbf{P} , $S(0,-a)=0$, while the maximum value is achieved at \mathbf{Q} , $S(0,a)=\pi L$. Therefore $0 \leq S \leq \pi L$.

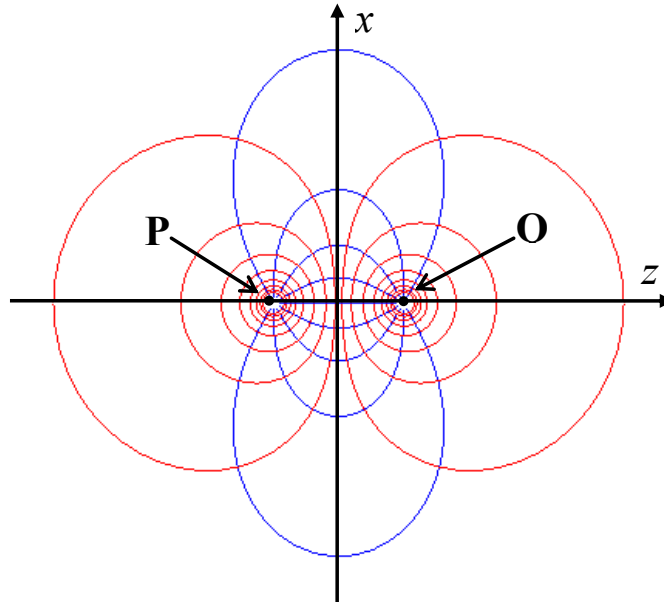


Figure 2. Section at $y=0$ showing the wavefronts (in red) and rays (in blue) associated with the 3D dipole lens. The system has rotational symmetry with respect to the z axis. Unlike in the 2D dipole lens (Figure 1), neither is it true that the ray trajectories are arcs of circumferences nor that the wavefront surfaces are spheres.

The refractive index distribution can be computed as:

$$n(\rho, z) = |\nabla S| = \sqrt{2} \frac{L}{a} \frac{\sqrt{a^4 + a^2(2\rho^2 + 6z^2 + s) + (\rho^2 + z^2)(\rho^2 + z^2 - s)}}{\left(\frac{s}{a}\right)^2 + 2(a^2 + \rho^2 + z^2 - s)} \quad (26)$$

Here $s = +\sqrt{a^4 + 2a^2(\rho^2 - z^2) + (\rho^2 + z^2)^2}$. Such a rotationally symmetric distribution is even in z (as expected by the symmetries of $V(\mathbf{r})$ and of $S(V)$) and is shown in Figure 3. At \mathbf{P} and \mathbf{Q} , $n = L/(\sqrt{2}a)$; at $(\rho, z) = (0, 0)$, $n = 2L/a$, which is the maximum value of n . For large values of $|\mathbf{r}|$, $n(\mathbf{r})$ is smaller than one (as also occurs in the Maxwell fish eye lens).

In order to calculate the field $U(S)$, first calculate $F(S)$ using Eq. (8) and (25):

$$F(S) = -(\ln V_S)_S = \frac{2}{L \tan\left(\frac{S}{L}\right)} = -\frac{2}{L} V(S) \quad (27)$$

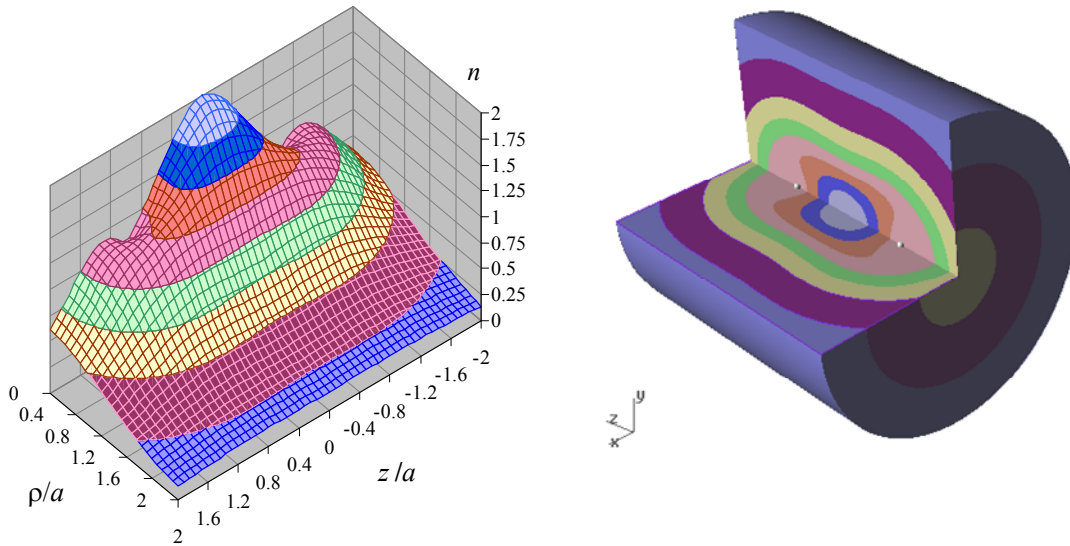


Figure 3. Normalized refractive index distribution $(a/L)n(\rho, z)$ of the selected example.

The field $U(S)$ is a solution of Eq. (5), which in this case is:

$$\frac{d^2U}{dS^2} + \frac{2}{L \tan\left(\frac{S}{L}\right)} \frac{dU}{dS} + k^2U = 0 \quad (28)$$

This is close to equation (18) except for the factor of 2. The general solution of equation (28) has the following simple closed form [12]:

$$U(S) = \frac{C_1 \sin(\kappa S) + C_2 \cos(\kappa S)}{\sin\left(\frac{S}{L}\right)} \quad (29)$$

Here C_1 and C_2 are arbitrary constants and:

$$\kappa = k \sqrt{1 + \left(\frac{1}{kL}\right)^2} \quad (30)$$

Note that that $\kappa \rightarrow k$ when $k \rightarrow \infty$. Select the particular solution $C_2 = 1/(4\pi a)$; $C_1 = i/(4\pi a)$, which leads to

$$U(S) = \frac{e^{i\kappa S}}{4\pi a \sin\left(\frac{S}{L}\right)} \quad (31)$$

The field can be expressed in cylindrical coordinates as $U(S(V(\rho, z)))$, so that from equations (31), (25) and (23):

$$U(\rho, z) = \frac{1}{4\pi a} \sqrt{1 + V^2(\rho, z)} e^{i\kappa L \left(\frac{\pi}{2} + \arctan(V(\rho, z))\right)} \quad (32)$$

Figure 4 shows the real part of $U(\rho, z)\exp(i\omega t)$ for $\omega t = 1.033\pi$, $a=1$, $L=1$, $\kappa=9.5$.

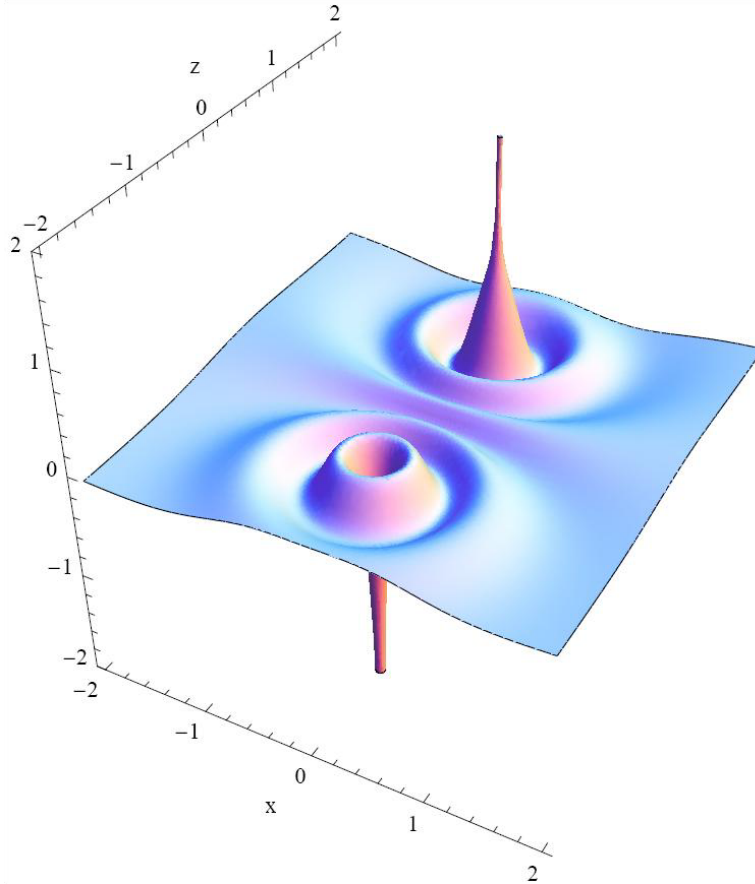


Figure 4. Real part of $U(S)$ of selected 3D dipole lens with $\omega t = 1.033\pi$, $a=1$, $L=1$, $k=9.5$ on the plane $y=0$. Due to the rotational symmetry, this graph also applies for any other plane containing the z axis.

The field diverges at both points \mathbf{P} and \mathbf{Q} , since at $S(\mathbf{P})=0$ and $S(\mathbf{Q})=\pi L$ the sine function vanishes in (31) and asymptotically behaves as:

$$U(S) \approx \frac{e^{i\kappa S}}{4\pi a(S/L)} \quad (\text{around } \mathbf{P})$$

$$U(S) \approx \frac{e^{i\kappa S}}{4\pi a(\pi - (S/L))} \quad (\text{around } \mathbf{Q})$$
(33)

This is because function S given by Eq. (25) approximates to:

$$S(\rho, z) \approx \frac{L}{a} \sqrt{\rho^2 + (z+a)^2} \quad (\text{around } \mathbf{P})$$

$$S(\rho, z) \approx \pi L - \frac{L}{a} \sqrt{\rho^2 + (z-a)^2} \quad (\text{around } \mathbf{Q})$$
(34)

Calling r the distance from a point (ρ, z) to \mathbf{P} and r' the distance to \mathbf{Q} , *i.e.*

$$r = \sqrt{\rho^2 + (z+a)^2} \quad r' = \sqrt{\rho^2 + (z-a)^2}$$
(35)

the asymptotic behavior of the field around \mathbf{P} and \mathbf{Q} can be written as:

$$U(\rho, z) \approx \frac{e^{i\kappa_1 r}}{4\pi r} \quad (\text{around } \mathbf{P})$$

$$U(\rho, z) \approx e^{i\kappa\pi L} \frac{e^{-i\kappa_1 r'}}{4\pi r'} \quad (\text{around } \mathbf{Q})$$
(36)

where:

$$\kappa_1 = \kappa \frac{L}{a}$$
(37)

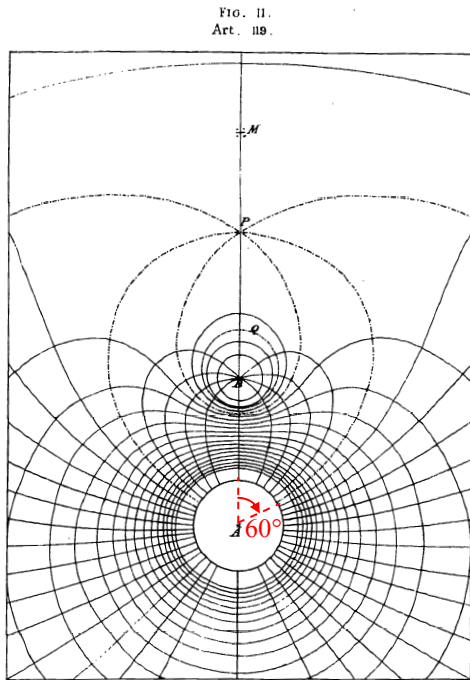
These expressions are identified as the field of a point source at \mathbf{P} emitting radiation and point drain at \mathbf{Q} receiving said radiation, so no flux is radiated towards infinity. In the absence of the drain at \mathbf{Q} , the field amplitude there will not diverge, because the wave will pass through the focus \mathbf{Q} , expand from it and converge back upon \mathbf{P} . In such a case, an three-dimensional Airy type pattern will appear at \mathbf{Q} [7]. This seems to indicate that both the amplitude at focus and the resolution capacity of the 3D dipole lens (and the Maxwell fish eye in two dimensions [5]) is limited by the wavelength. However, we expect that using subwavelength absorbers as detectors, to emulate the point drain, it will be possible to resolve two point sources separated by a distance much smaller than the wavelength.

5. DESIGNS WITH MULTIPLE POINT SOURCES OR DRAINS

The design procedure for refractive indices described in section 2.2 can be applied to any harmonic function. Therefore, with the help of basic knowledge of electrostatic, we can easily compute, for instance, refractive index distributions that take focus the scalar waves emitted from one or multiple point sources towards one or several point drains.

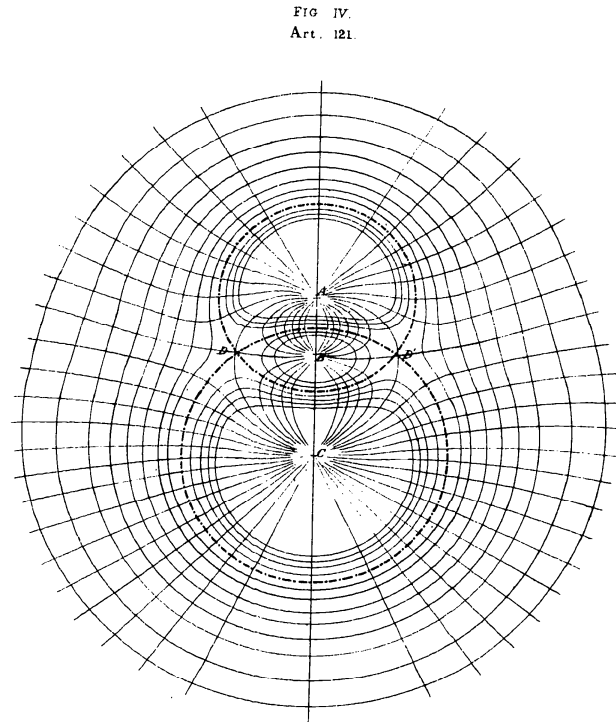
Two beautiful examples are shown in Figure 5. These are the field lines and equipotential surfaces (rays and wavefronts for us) calculated by Maxwell and published in 1873 [15]. The example on the left is a positive charge at A four times a negative charge at B . If the positive charge is consider as the source in our problem, we see in the figure that the power emitted from A in the solid angle $\theta < 60^\circ$ is coupled to fill the full solid angle around the drain at B (the $\theta = 60^\circ$ field line is the one passing through the equilibrium point P). This defines, as expected, exactly $1/4$ of the total solid angle, *i.e.*, $2\pi(1 - \cos\theta) = 1/4(4\pi)$. The remaining $3/4$ is emitted towards the infinity. In the example on the right, two unequal positive charges and a negative one are aligned. Both positive charges, seen are point sources, will transfer a fraction of their emitted power to fully feed the drain.

Note that equation (25) and (32) also apply to these examples (L and a are normalization constants with no specific meaning here): the first to calculate the eikonal function S from V (and then $n(\mathbf{r})$ as $|\nabla S|$), and the second to calculate the field. Note that the resulting refractive index distribution will general not be rotational symmetric.



Lines of Force and Equipotential Surfaces.

$A = 20$ $B = -5$ P , Point of Equilibrium. $AP = 2 AB$
 Q , Spherical surface of Zero potential.
 M , Point of Maximum Force along the axis.
The dotted line is the line of Force $\nabla = 0.1$ thus.



Lines of Force and Equipotential Surfaces.

$A = 15$ $B = -12$ $C = 20$.

Figure 5. Example of field lines and equipotential surfaces (rays and wavefronts for us) with several unequal charges calculated by Maxwell and published in 1873.

6. CONCLUSIONS

We have found non-trivial isotropic non-homogenous refractive-index distributions that propagate Helmholtz fields $U(\mathbf{r})$ exactly on eikonals in that medium, in the sense that that $U(\mathbf{r})=U(S(\mathbf{r}))$, where $S(\mathbf{r})$ is a particular solution of the eikonal equation in that medium.

As an example, we have found a (positive) refractive index distribution $n(\mathbf{r})$, the “3D dipole lens”, which in three dimensions perfectly focuses a point source at \mathbf{P} , emitting a Helmholtz scalar wave field, onto a point drain at \mathbf{Q} . To our knowledge this is the first example of such a system with a positive refractive index. Apart from the difficulty of making the 3D dipole lens (because eventually $n(\mathbf{r})$ goes below 1), they have a clear theoretical interest. Perfect focusing of Helmholtz fields in 3D is particularly relevant to acoustics (for example, to ultrasound imaging), turning the sound waves of an explosion into an implosion.

The cylindrical Maxwell fish eye lens in two dimensions has shown to be a particular example of the “2D dipole lens”, although it has the very remarkable property that produces the perfect focusing for the point source \mathbf{P} located in any arbitrary position, which makes it a perfect imaging device in two dimensions [5]. We have also shown that the spherical Maxwell fish eye lens does not belong to the family of refractive indices discussed here, that is, there is no solution of the Helmholtz equation in three dimensions that propagates exactly on eikonals in the spherical Maxwell fish eye medium.

The constructive procedure developed here opens the possibility of designing other interesting novel refractive-index distributions that propagate fields exactly on eikonals. For instance, perfect scalar wave focusing from a point source into multiple point drains (or from multiple point source into a single point drain) is obtained when the harmonic function $V(\mathbf{r})$ is selected as that produced by several electric charges.

ACKNOWLEDGMENTS

The authors thank the Spanish Ministries MCEI (Engineering Metamat. CSD2008-00066, DEFFIO: TEC2008-03773, Sigmasoles PSS-440000-2009-30;), and MITYC (OSV: TSI-02303-2008-52), and the Madrid Regional Government and UPM (Q090935C-019) for the support given in the preparation of the present work.

REFERENCES

- [1] M. Born, E. Wolf, [Principles of Optics], 5th ed, Pergamon, Oxford, (1975)
- [2] S. Cornbleet, [Microwave and Geometrical Optics], Academic, London, (1994)
- [3] Juan C. Miñano, "Perfect imaging in a homogeneous three-dimensional region," Opt. Express **14**, 9627-9635 (2006) <http://www.opticsinfobase.org/oe/abstract.cfm?URI=oe-14-21-9627>.
- [4] J. B. Pendry, "Negative refraction makes a perfect lens", Phys. Rev. Lett. 85: 3966, (2000)
- [5] U. Leonhardt, "Perfect imaging without negative refraction", New Journal of Physics **11** (2009)
- [6] U. Leonhardt, T.G. Philbin, "Perfect imaging with positive refraction in three dimensions", Phys. Rev. A 81, 011804 (2010)
- [7] P. Benítez, J.C. Miñano, and J.C. González, "Perfect focusing of scalar wave fields in three dimensions," Opt. Express **18**, 7650-7663, (2010) <http://www.opticsinfobase.org/oe/abstract.cfm?URI=oe-18-8-7650>.
- [8] M. A. Alonso, G. Forbes, "Stable aggregates of flexible elements give a stronger link between rays and waves," Opt. Express **10**, 728-739 (2002). <http://www.opticsinfobase.org/oe/abstract.cfm?URI=oe-10-16-728>
- [9] O. N. Stavroudis, [The Mathematics of Geometrical and Physical Optics], Willey-VCH, Weinheim, (2006)
- [10] R.K. Luneburg, [Mathematical Theory of Optics], University of California Press, Los Angeles (1964)
- [11] P.M. Morse, H Feshbach, [Methods of Theoretical Physics], New York, McGraw-Hill, (1953)
- [12] A. D. Polyanin, V. F. Zaitsev, [Handbook of Exact Solutions for Ordinary Differential Equations], 2nd Edition, Chapman & Hall/CRC, Boca Raton, (2003). It also coincides with the change of variables $S'=S/L+\pi/2$ in the equation described in <http://eqworld.ipmnet.ru/en/solutions/ode/ode0235.pdf>.
- [13] http://www.youtube.com/watch?v=bG9XSY8i_q8
- [14] <http://www.mathcurve.com/courbes2d/cayleyovale/cayleyovale.shtml>
- [15] J C Maxwell, [A treatise on electricity and magnetism, Vol I], Oxford at the Clarendon Press, London, 428-430, (1873)